**Stem Cell Reports, Volume *9***

## Supplemental Information

# Network-Based Genomic Analysis of Human Oligodendrocyte Progenitor Differentiation

**Suyog U. Pol, Jessie J. Polanco, Richard A. Seidman, Melanie A. O'Bara, Hani J. Shayya, Karen C. Dietz, and Fraser J. Sim**

## Dugas; Rat OPC differentiation

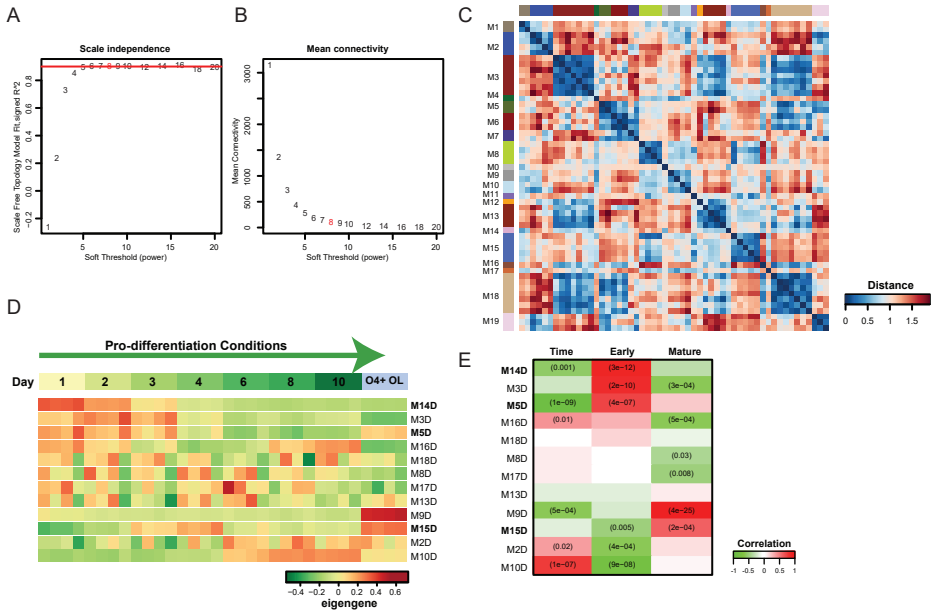


## Cahoy; Mouse isolated neural populations

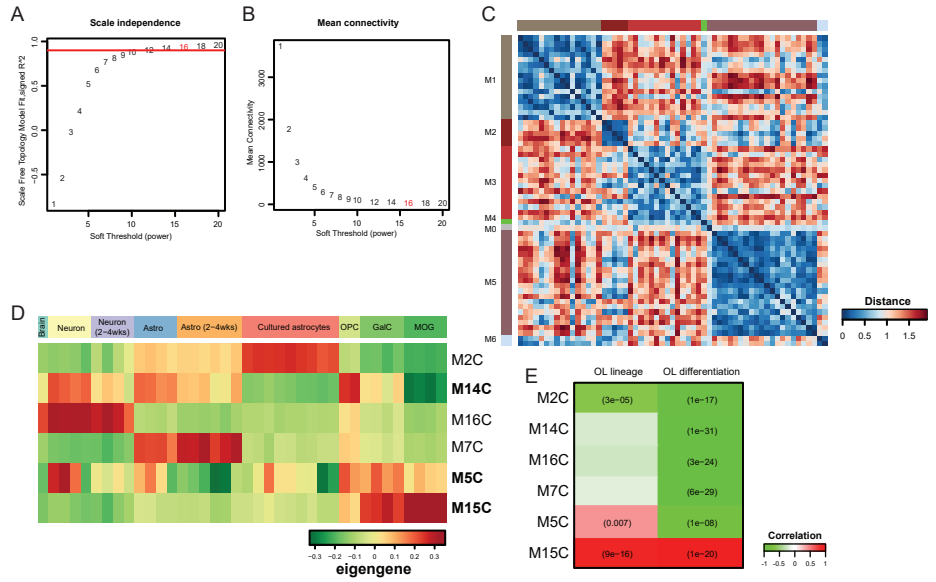


## Abiraman; Human isolated OPCs

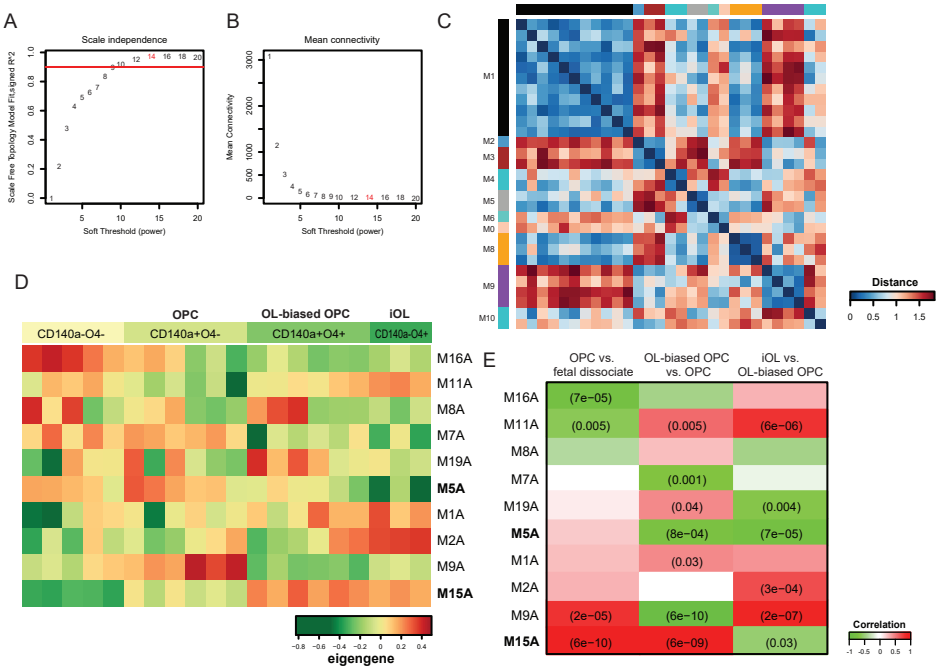

# Figure S2

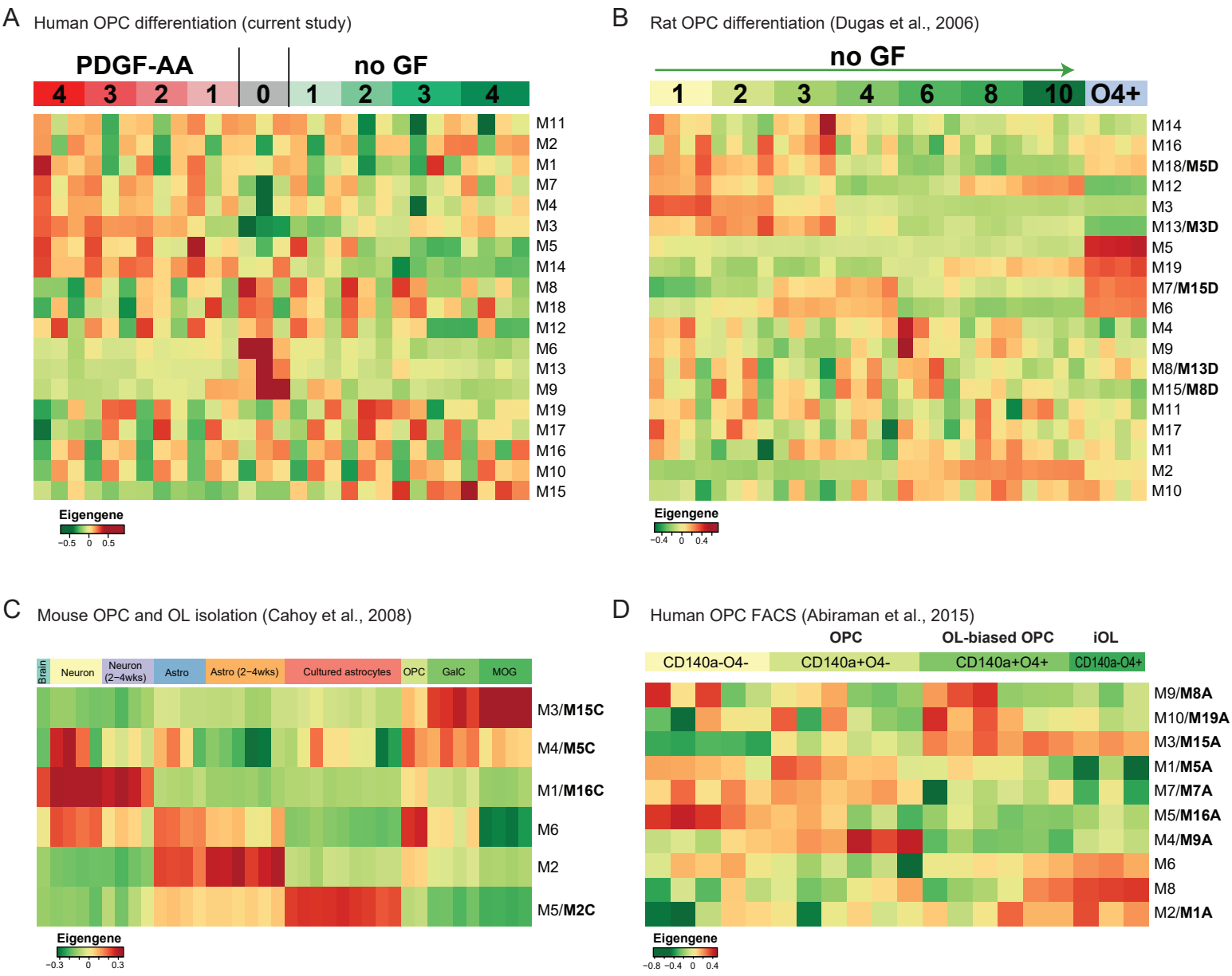
A
Human OPC differentiation (current study)
PDGF-AA
no GF
4 3 2 1 0 1 2 3 4
M11 M2 M1 M7 M4 M3 M5 M14 M8 M18 M12 M6 M13 M9 M19 M17 M16 M10 M15
Eigengene
−0.5 0 0.5
B
Rat OPC differentiation (Dugas et al., 2006)
no GF
1 2 3 4 6 8 10 O4+
M14 M16 M18/M5D M12 M3 M13/M3D M5 M19 M7/M15D M6 M4 M9 M8/M13D M15/M8D M11 M17 M1 M2 M10
Eigengene
−0.4 0 0.4
C
Mouse OPC and OL isolation (Cahoy et al., 2008)
Brain
Neuron
Neuron (2−4wks)
Astro
Astro (2−4wks)
Cultured astrocytes
OPC
GalC
MOG
M3/M15C M4/M5C M1/M16C M6 M2 M5/M2C
Eigengene
−0.3 0 0.3
D
Human OPC FACS (Abiraman et al., 2015)
OPC
OL-biased OPC
iOL
CD140a-O4-
CD140a+O4-
CD140a+O4+
CD140a-O4+
M9/M8A M10/M19A M3/M15A M1/M5A M7/M7A M5/M16A M4/M9A M6 M8 M2/M1A
Eigengene
−0.8 −0.4 0 0.4

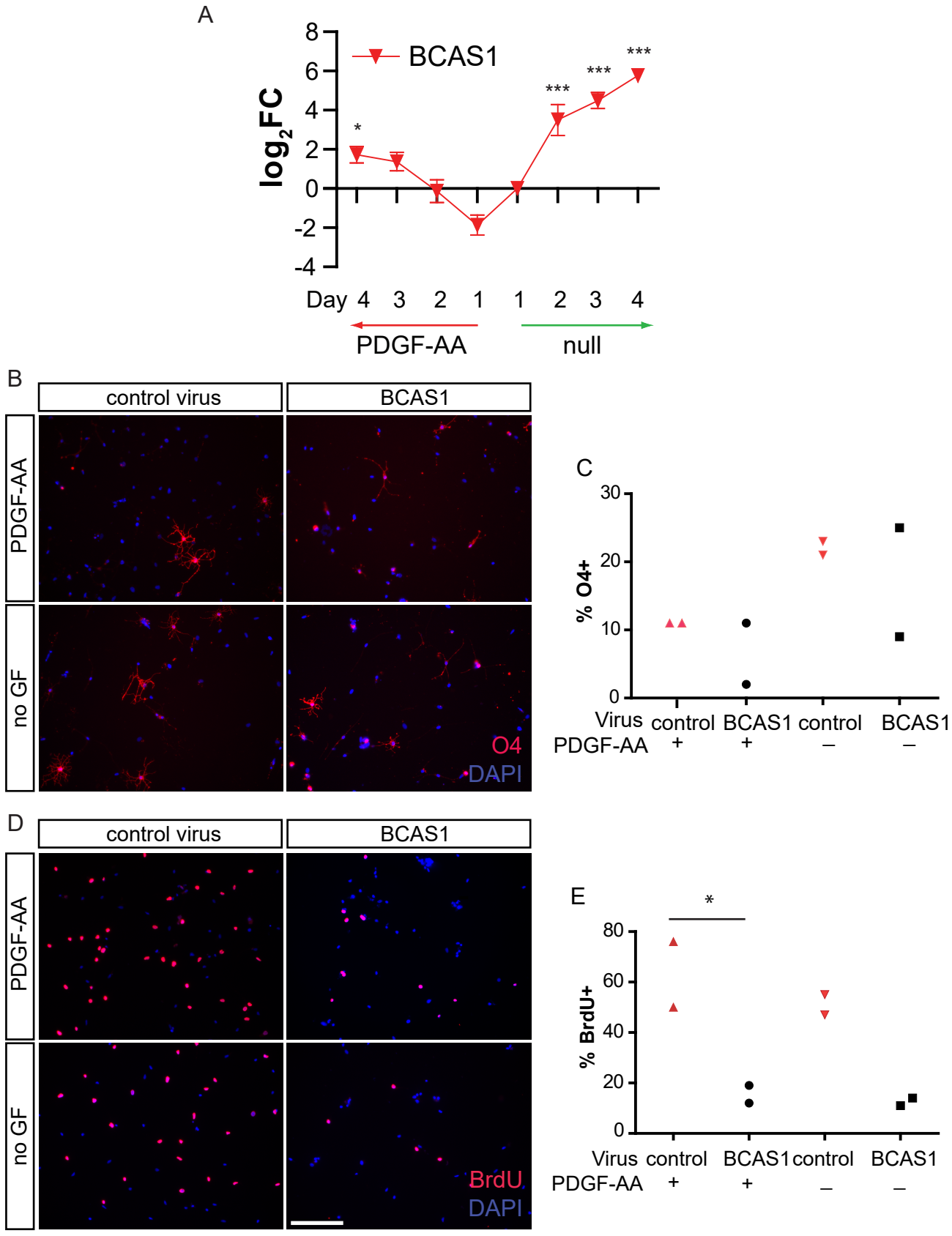
A
BCAS1
log2FC
8
6
4
2
0
-2
-4
*
***
***
***
Day 4 3 2 1 1 2 3 4
PDGF-AA
null
B
control virus
BCAS1
PDGF-AA
no GF
O4
DAPI
C
% O4+
30
20
10
0
Virus control BCAS1 control BCAS1
PDGF-AA + + – –
D
control virus
BCAS1
PDGF-AA
no GF
BrdU
DAPI
E
*
% BrdU+
80
60
40
20
0
Virus control BCAS1 control BCAS1
PDGF-AA + + – –

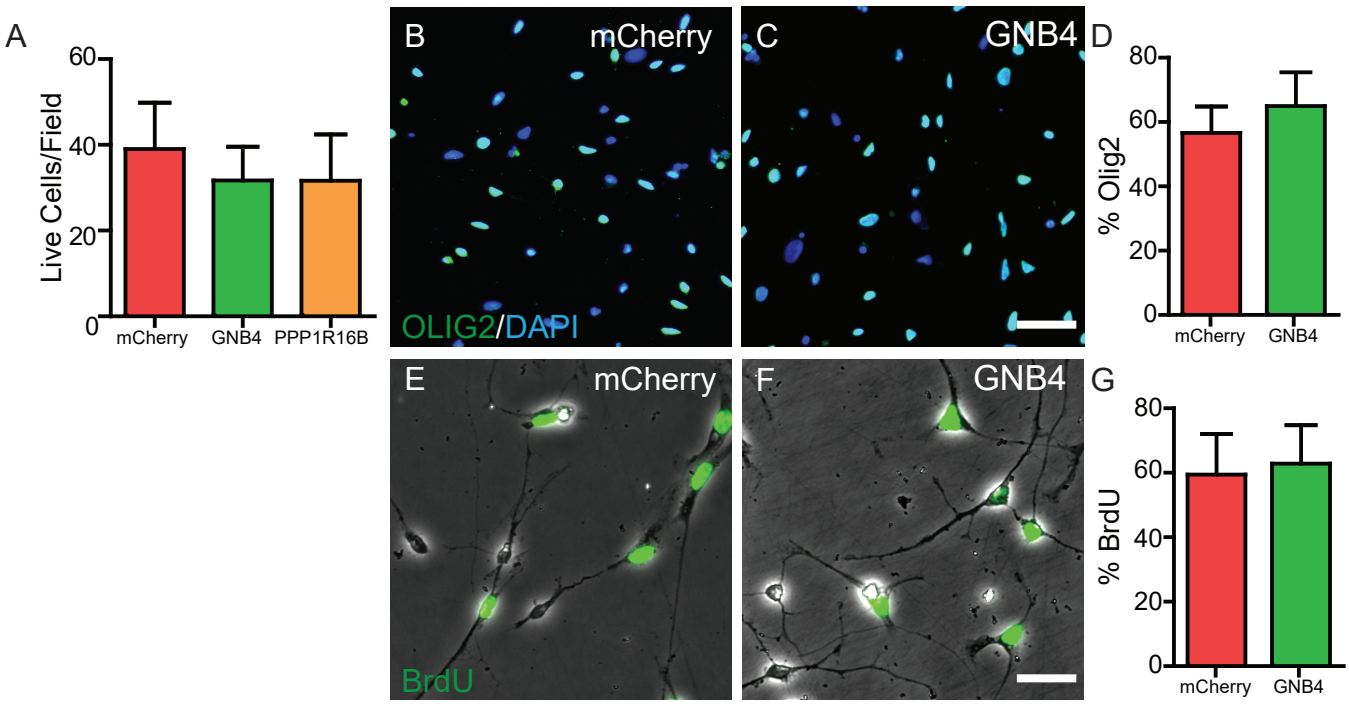
A
Live Cells/Field
60
40
20
0
mCherry
GNB4
PPP1R16B
B
mCherry
OLIG2/DAPI
C
GNB4
D
% Olig2
80
60
40
20
0
mCherry
GNB4
E
mCherry
BrdU
F
GNB4
G
% BrdU
80
60
40
20
0
mCherry
GNB4

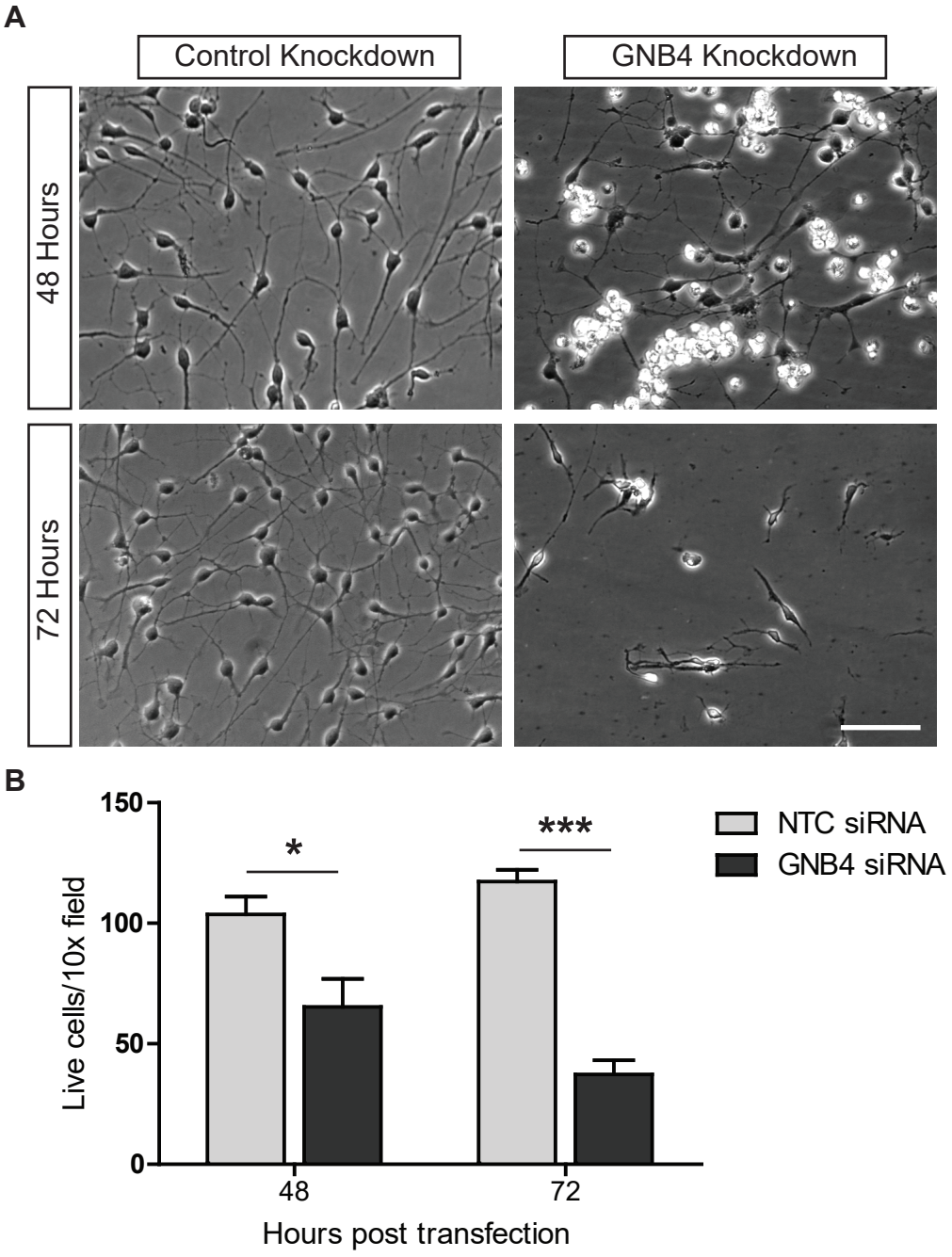
A
Control Knockdown
GNB4 Knockdown
48 Hours
72 Hours
B
150
100
50
0
Live cells/10x field
*
***
NTC siRNA
GNB4 siRNA
48
72
Hours post transfection

A

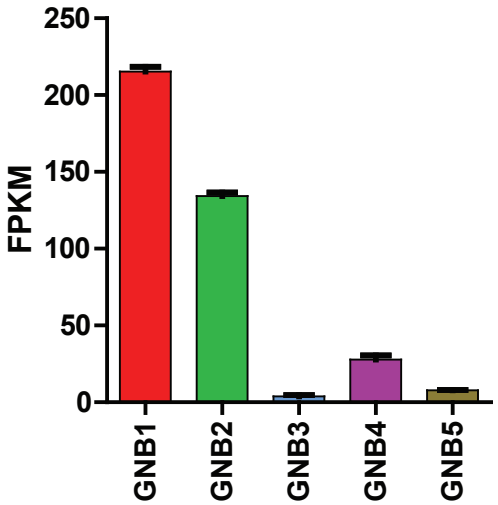


B

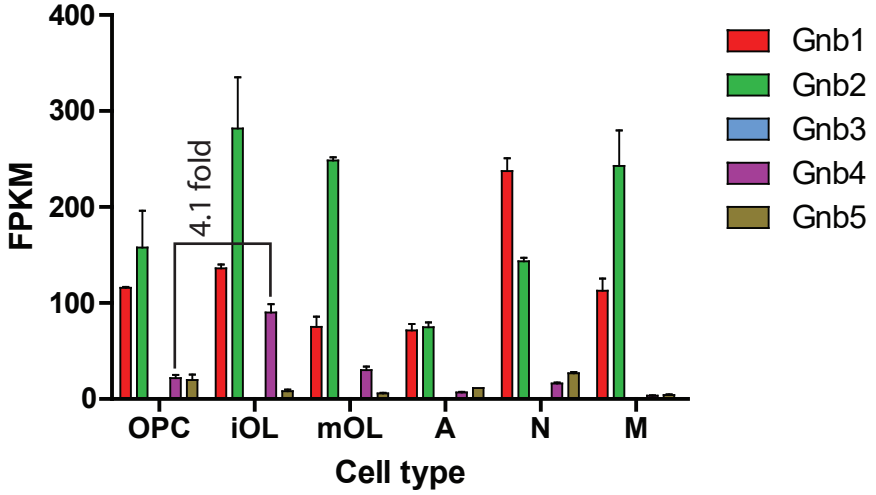


C

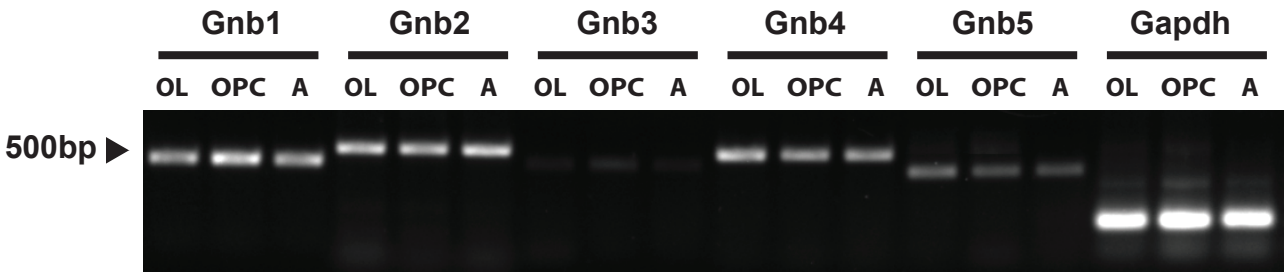


| Gene | Forward | Reverse | Product Size(bp) |
|---|---|---|---|
| Gnb1 | CTGGCAGGACATACAGGTTATC | TGAGTGCATCCCAGACATTAC | 487 |
| Gnb2 | GGACAGCTACACCACTAACAA | TGTTGTCGTGGGAATACATGAG | 560 |
| Gnb3 | CTCGGCTCACACAGGTTATC | CTTCAGAGAGTCCCAGACATTG | 487 |
| Gnb4 | GGGATACGATTCCAGGCTACTA | ACCAGTGGCAAAGGCATATC | 544 |
| Gnb5 | GCTTGTGGTGGTCTGGATAATA | ATCTGCCCTCAGGTCATAGA | 453 |
| Gapdh | GTGAAGGTCGGAGTGAACGG | CCTGGAAGATGGTGATGGGC | 115 |

**Figure S7**

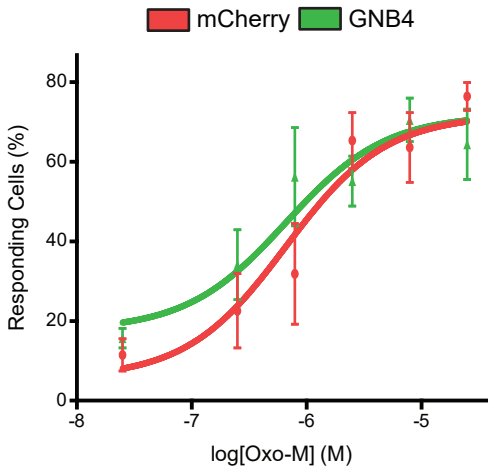

## SUPPLEMENTAL FIGURE LEGENDS

**Figure S1 (related to Figure 2). Summary of Weighted gene coexpression network analysis in cultured rat OPCs, isolated mouse cell populations, and PDGFRA/O4 sorted hOPCs.**

**For each data set:**
**A,** fit of power-transformed gene-pairwise Pearson correlation with a scale free topology at each soft threshold. **B**, mean connectivity as a function of soft threshold. The power was set to 8 to transform the data to best fit with scale-free topology (marked in red). **C**, heatmap of Pearson correlations between unmerged module eigengenes. **D**, expression profiles of merged module eigengene. Merged modules were labeled according to the greatest overlap with modules identified in the profile of differentiating human OPCs (labeled with a 'D' suffix). **E**, correlation of module eigengenes with experimental parameters.

The power (soft threshold) was set to 8 (rat OPC; Dugas), 16 (mouse; Cahoy), 14 (hOPC; Abiraman).

Merged modules were labeled with a 'D', 'C', or 'A' suffix, for Dugas, Cahoy, and Abiraman datasets respectively.

Correlation with experimental parameters included:

Dugas: time and expression in $O4^+$ oligodendrocytes.

Cahoy: oligodendrocyte lineage and differentiation (i.e. up from $PDGF\alpha R^+$ OPC to $MOG^+$ OLG).

Abiraman: $PDGFRA^+$ OPC vs. $PDGFRA^-$ dissociate, $PDGFRA^+O4^+$ biased OPC vs. $PDGFRA^+O4^-$, and $PDGFRA^-O4^+$ immature oligodendrocyte (iOL) vs. $PDGFRA^+O4^+$ biased OPC

**Figure S2 (related to Figure 5). Module eigengenes from four data sets.** Heatmaps of every module eigengene expression in the four data sets. Rat (**B**), mouse (**C**) and sorted hOPC (**D**), modules are numbered per the WGCNA overlap analysis. If significant overlap was found, the matching module name is also provided.

**Figure S3 (related to Figure 5). The effect of BCAS1 over-expression on human $PDGFRA^+$ OPCs. A,** real-time quantitative PCR analysis of BCAS1 mRNA expression during human OPC differentiation (mean ± SEM $\log_2$ fold change relative to day 1 conditions, n=4 human samples). * and *** indicate posttest $p < 0.05$ and 0.001, respectively; Tukey's posttest vs. day 1 noGF conditions). **B-E**, hOPCs were infected with retroviruses expressing BCAS1 or an empty vector, and allowed to grow in the presence or absence of PDGF-AA (20 ng/ml) for 4 days. BrdU was pulsed 24 hours prior to fixation and cultures immunostained for O4 (**B**) and BrdU (**D**). Quantification and statistical analysis of O4 (**C**) and BrdU (**E**) proportions. As expected, growth media had a significant effect on $O4^+$ oligodendrocyte differentiation ($p<0.05$, significant effect of media conditions ($F=34.89$ [1,2]), 2-way ANOVA). BCAS1 virus did not affect the percentage of $O4^+$ cells ($p>0.05$, effect of virus ($F= 0.57$ [1,2], 2-way ANOVA). However, BCAS1 over-expression significantly reduced the proportion of dividing $BrdU^+$ hOPCs (2-way ANOVA, $F=25.2$ [1,2], $p=0.037$). Scale: 200 µm.

**Figure S4 (related to Figure 5). GNB4 over-expression does not alter OPC proliferation or OLIG2 lineage status.** hOPCs were infected with lentivirus overexpressing mCherry (Control) or GNB4 over-expressing virus, and allowed to differentiate for 4 days. Quantification after 4 days

showed no significant effect of GNB4 or PPP16R1B on live cell number (**A**), the proportion of Olig2$^+$ oligodendrocyte lineage cells (**B-D**), or the proportion of proliferative BrdU$^+$ cells (**E-G**) ($p > 0.05$, n = 4 fetal samples, unpaired t-test). Scale: 100µm (**B, C**), 50µm (**E, F**).

**Figure S5 (related to Figure 5). GNB4 KD induces rapid hOPC death.** hOPC were transfected with siRNAs targeting GNB4 or a scrambled control, and allowed to differentiate in the absence of mitogens (**A**). **Top**, Micrographs of hOPC in culture 48 hours after mitogen removal. GNB4 knockdown hOPC show reduced viability, observed as a reduction in cell number, rounded morphology, clumping of unviable cells. **Bottom**, Micrographs of hOPC following media change, 72 hours after mitogen removal. **B**, GNB4 knockdown hOPCs show substantially reduced cell number. *, *** indicate $p < 0.05$, 0.001, n = 3, two-way ANOVA with Bonferroni post-test. *Scale: 100µm.

**Figure S6 (related to Figure 6). GNB subtype expression in OPCs. A,** RNA-seq analysis of human OPCs indicates that GNB1/2 are more abundant in progenitors prior to differentiation. GNB3 was essentially not detected (mean ± SEM, n = 3 fetal human samples). **B**, RNA-seq analysis of mouse OPCs and OLGs (Zhang et al., 2014) indicates that GNB4 is strongly up-regulated during differentiation and becomes as abundant as GNB1/2 in immature oligodendrocytes, i.e., the equivalent stage to day 4 differentiating hOPCs (mean ± SEM, n = 2). **C**, RT-PCR analysis of G-protein $\beta$ subunit expression in rat CG-4 OPCs (repeated three times, representative image shown). OPCs were either maintained in PDGF-AA/FGF conditions (OPC) or induced to differentiate into oligodendrocytes (OL) or astrocytes (A) prior to RNA extraction. RT-PCR revealed abundant expression of rat Gnb1/2/4 at all stages, whereas Gnb3/5 transcripts were not abundant, consistent with the mouse RNA-seq data. As such, $G_{\beta 4}$ is abundantly expressed by mouse, rat, and human immature oligodendrocytes. The primer sequences used are shown below the gel image.

**Figure S7 (related to Figure 6). $G_{\beta 4}$ over-expression does not affect muscarinic activation.** Fetal PDGF$\alpha$R$^+$ hOPCs were cultured and infected with intracellular [$Ca^{2+}$] reporter GCaMP6s. Following infection with GNB4- or mCherry over-expression lentivirus, time-lapse microscopy of $Ca^{2+}$ response after muscarinic agonist, Oxo-M, treatment was recorded and analyzed. The percentage of responding cells after Oxo-M addition is shown. GNB4 had no significant effect on $EC_{50}$ for response to muscarinic stimulus ($LogEC_{50}$ = -5.9 ± 0.2 vs. -6.5 ± 0.3 for mCherry and GNB4, respectively, $p > 0.05$, n > 90 cells per condition from two individual human samples).

**SUPPLEMENTAL TABLES**

**Table S1. See excel spreadsheet.**

**Table S2. See excel spreadsheet.**

**Table S3: Antibodies used.**

| Antibody | Host | Dilution | Source | Catalog Number |
|---|---|---|---|---|
| O4 | Mouse IgM | 1:25 | Dr. James Goldman (Columbia University) | n/a |
| Olig2 | Rabbit IgG | 1:2000 | Millipore Sigma | AB9610 |
| Human Nuclei (hNA) | Mouse IgG1 | 1:100 | Millipore Sigma | MAB1281 |
| MBP | Rat | 1:400 | Abcam | AB7349 |
| CC1 | Mouse | 1:50 | EMD Chemicals | OP80 |
| Ki67 | Rabbit IgG | 1:250 | ThermoFisher Scientific | RM-9106-S1 |
| GFAP | Mouse IgG1 | 1:800 | BioLegend (Covance) | SMI-21R |
| BrdU | Rabbit IgG | 1:1000 | Bio-Rad AbD (Serotec Inc) | MCA2060 |

**Table S4: Oligonucleotide primers for real-time quantitative PCR.**

| Gene | Primer Sequence (5' -> 3') | |
|---|---|---|
| hsGAPDH | Fwd: | GTGAAGGTCGGAGTCAACGG |
| | Rev: | CCTGGAAGATGGTGATGGGA |
| hsMBP | Fwd: | GGCAGAGCGTCCGACTATAAA |
| | Rev: | CGACTATCTCTTCCTCCCAGCTT |
| hsCSPG4 | Fwd: | GAGGACAGCTGGAGCTCTAGGGT |
| | Rev: | AGGCCTGGGACCAAAGCGGA |
| hsBCAS1 | Fwd: | AGGCCTGGGACCAAAGCGGA |
| | Rev: | ACCTGGTGGGAACCGTGCTGA |
| hsGNB4 | Fwd: | AAGTGGGCGTCTCTTGTTGGC |
| | Rev: | CCAGCAAGGACACCTGCACGAT |
| hsPPP1R16B | Fwd: | AGGACCCTAACCCCAGGCTGG |
| | Rev: | GGAGCCCGGAGGCCATTCTC |

## SUPPLEMENTAL EXPERIMENTAL PROCEDURES

*Cell and Tissue Samples*

Fetal brain samples (18-22 wk gestational age) were obtained from patients who consented to tissue use under protocols approved by the State University of New York at Buffalo Institutional Review Board. Cortical tissue, including ventricular and subventricular zones, was dissociated and prepared as previously described (Windrem et al., 2002) and cultured in serum-free media with 10 ng/ml FGF2 (PeproTech, Inc., Rocky Hill, NY, USA) (as detailed in Sim et al., 2011).

*Magnetic isolation of human PDGFRA$^+$ OPCs*

Magnetic sorting of PDGFRA was performed as described (Sim et al., 2011). Briefly, cells were recovered and stained with PDGFRA PE-conjugated purified mouse $IgG2_a$ antibody (BD Pharmingen, San Diego, CA). Cells were washed and rat anti-mouse $IgG_{2a+b}$ secondary antibody was added according to the manufacturer's instructions (Miltenyi Biotech, Auburn, CA). Magnetic sorting was performed using LS column selection and a sample of positive cells collected for subsequent flow cytometry-based analysis of purity.

*Immunocytochemistry*

Cultures were exposed continuously to 10 µg/ml BrdU beginning 24 hours before fixation. O4 supernatant (gift of Dr. James Goldman, Columbia University) was applied to live cultures for 30 minutes at 37ºC (1:25 dilution) pre-fixation. Cultures were washed and fixed in 4% paraformaldehyde and immunostained for OLIG2 (1:2000, Millipore, Billerica, MA) or BrdU (1:1000, Serotec, Raleigh, NC). Secondary antibodies, Alexa-488, -647 conjugated goat anti-rabbit IgG, mouse IgM or rat IgG antibodies were used at a dilution of 1:500 (Invitrogen, Carlsbad, CA). The number of O4, OLIG2 and BrdU stained and unstained cells were quantified in 10 random fields, representative of over 250 random cells.

*Real-time RT-PCR analyses*

PDGFRA$^+$ hOPCs were plated onto 35 mm tissue culture plates coated with poly-L-ornithine and laminin at $1\times10^5$ cells/ml in serum-free media as described above. mRNA was isolated using an E.Z.N.A Total RNA Kit I (Omega Bio-Tek, Norcross, GA) according to manufacturer's protocols and cDNA prepared (SuperScript III Kit; Invitrogen, Carlsbad, CA). Human-specific primers for SYBR green-based PCR were designed using Primer Express (v1, Applied Biosystems, Foster City, CA) (**Table S4**). Samples were run in duplicates for real-time PCR (MyiQ; Bio-Rad, Hercules, CA), and gene expression calculated by $\Delta\Delta C_t$ analysis using the primer efficiency, as previously described (Pfaffl, 2004). Gene expression was normalized to the control gene GAPDH. Statistical significance was tested on $\log_2$-transformed data using repeated measures 1-way ANOVA followed by Tukey's posttest (GraphPad Prism version 5.01 software).

*Microarray analysis*

Prior to array analysis, mRNA was amplified using NuGEN WT-Ovation Pico RNA amplification system according to manufacturer's instructions. Amplified product was hybridized onto Illumina HT-12v3 bead arrays according to manufacturer's instructions (Illumina). All microarray data were analyzed using R/Bioconductor (Gentleman et al., 2004). The complete analysis code is available on request (fjsim@buffalo.edu). The complete microarray data are available at NCBI GEO GSE36431 and may be directly browsed via FINDdb (www.FindDB.org). Briefly, raw data were loaded using the *lumi* package (Du et al., 2008), samples were background corrected, vsn transformed/normalized, and poor quality data were filtered using a detection call p-value cutoff of 0.01. Exploratory analysis was then performed using 3dPCA and hierarchical clustering - *analysisPipeline* package, Sim et al. (2011). A custom annotation package (*nuID.combined.db*) was developed to improve annotation. This package combined annotations

from Agilent, Ensembl (Durinck et al., 2005), and *lumiHumanAll.db* (Du et al., 2008). The expression of genes associated with OPC fate and oligodendrocyte differentiation were visualized following normalization to day zero median expression (heatmap.2, *gplots*).

For cross-species analysis, we compiled raw data from various published data sets. The expression profiles of freshly isolated PDGFRA and O4 FACS-isolated hOPC cells was pre-processed exactly as described above (Abiraman et al., 2015). The profiles of differentiating rat $A2B5^+$ OPC data (GSE9566) (Dugas et al., 2006) and freshly isolated mouse cells, including OPCs (GSE9566) (Cahoy et al., 2008) were normalized by justRMA (*Affy*) and non-informative probe sets filtered (*farms*) (Hochreiter et al., 2006). Affymetrix microarray data were annotated using Bioconductor packages *rgu34abc* and *mouse4302*, and gene expression data matrices were generated using nsFilter (*genefilter*).

*Weighted gene coexpression network analysis (WGCNA)*

WGCNA was performed using the R/Bioconductor package (Langfelder and Horvath, 2008) following the method described in Konopka et al. (2009). A total of 12,494 genes were included in the hOPC differentiation analysis. Similar analyses were performed with PDGFRA/O4 hOPCs (12,404 genes), mouse cell-type specific (11,202 genes), and rat OPC differentiation (11,091 genes) data. Module membership was defined as the intramodular connectivity representing the sum of Pearson correlations to each gene in the module. Characterization of module function was first performed by analysis of the module eigengene which is defined as the first principle component of the expression profiles of its constitutive genes. The expression profile of each module eigengene was correlated with experimental parameters specific to each data set. For example, we correlated the hOPC differentiation data module eigengenes with both time *in vitro* and media conditions to identify modules whose expression was up-regulated in differentiating conditions.

The degree of species conservation between WGCNA-derived modules was analyzed by hypergeometric analysis of module overlap, as described in Oldham et al. (2008). Briefly, human Entrez ID homologs of rat and mouse genes were found in each data set using a combination of NCBI homologene, ensembl homologs found using *biomaRt*, and Bioconductor homology packages - *analysisPipeline* package (Sim et al., 2011). Significance was calculated using a one-sided hypergeometric test of overlapping genes in each module (using the top $50^{th}$ percentile of connected genes in each module), and corrected for multiple comparisons by false discovery rate (q-value < 0.1). Modules from different networks with significant overlap were assigned the same number, with the suffix denoting the dataset [e.g. M15 for hOPC differentiation, M15D for Dugas et al. (2006), M15C for Cahoy et al. (2008), and M15A for Abiraman et al. (2015)]. If a module overlapped with more than one module from the hOPC differentiation dataset, we assigned the module number based on the lowest p-value.

Over-representation of specific gene ontology terms was performed using *topGO* (Alexa et al., 2006). Module hub genes were defined as the top 30 genes with highest intramodule connectivity, i.e. the sum of the Pearson correlation to all other module members. These were visualized as a graph using *Rgraphviz.*

*Viral cloning and packaging*

Retroviral BCAS1-IRES-GFP and control MIG-GFP virus were used at 2 multiplicity of infection (MOI) (gift of Dr. Magdalena A. Petryniak, Oregon Health & Science University). To generate lentiviral over-expression vectors, the coding region of each gene was PCR-amplified from fetal human brain cDNA and cloned into a lentiviral expression plasmid as described previously (Wang et al., 2014) (pTRIP-EF1α; gift from Abdel Benraiss, University of Rochester, Rochester, NY). Virus was prepared by $CaPO_4$-based transfection as described in Jordan et al. (1996). Collected virus was then concentrated using high-speed centrifugation (50,000 g, 90 min; Beckman Coulter Rotor JA-25.5). Viral titers were measured using real-time RT-PCR for

expression of WPRE (Geraerts et al., 2006) and compared to titers determined using flow cytometry with TRIP-mCherry virus. hOPCs were infected one day after seeding at one MOI and the infection was stopped at 24 hours by exchange of culture medium.

*siRNA-mediated gene knockdown*

siRNA molecules were obtained from ThermoFisher Scientific, three targeting GNB4 (HSS126985, HSS126987, HSS184233), and a scrambled negative control (#12935112). hOPCs were seeded as previously described at a density of $10^5$ cells/ml onto 48-well plates. 24 hours later, siRNA were transfected, combined or individually, at a total concentration of 100μM siRNA, using Lipofectamine RNAiMAX transfection reagent (ThermoFisher Scientific). Knockdown efficiency was determined by qPCR, 48 hours post-transfection.

*Cloning of LV-EF1a:GCaMP6s*

We PCR/TOPO cloned the coding region of GCaMP6s from pLP-CMV-GCaMP6s-CAAX (AddGene, #52228)(Tsai et al., 2014) into pCR2.1 TOPO4 plasmid (Invitrogen). The GCaMP6s fragment was then subcloned using unique 5' SpeI and 3' PspXI restriction sites into lentiviral pTRIP-EF1a (derived from pTRIP-EF1a, in Sevin et al., 2006) (gift of Abdel Benraiss, University of Rochester). Lentiviruses were prepared as described above. Viruses were tittered on the basis of matched mCherry-expressing virus using flow cytometry for mCherry fluorescence and directly compared to GCaMP6s virus using real-time quantitative PCR for the WPRE sequence (Geraerts et al., 2006). GCaMP6s expression was confirmed using CHO-$M_3$R expressing cells (gift of Dr. Jurgen Wess) by fluorescence imaging following addition of carbachol or $CaCl_2$. For all imaging experiments, hOPCs were infected at one MOI for 24 hours followed by complete media replacement. One hour prior to imaging, media was replaced with phenol red-free media.

*Calcium imaging using LV-EF1a:GCaMP6s*

All calcium imaging experiments were performed at 10x magnification using an Olympus IX51 with a Prior XYZ stage equipped with a Hamamatsu ORCA-ER camera using a 1x TV lens. All phase images and fluorescent time-lapse acquisitions were performed at room temperature and captured using μManager (Edelstein et al., 2010a). Oxotremorine-M (Tocris) was thawed immediately prior to each experiment. Two fields per preparation were imaged for each condition, at 2-second intervals for 10-12 minutes. Drug addition occurred 1 min after the start of imaging. Phase images were used to generate regions of interest corresponding to the soma of every cell by thresholding and supervised analysis. Rolling ball subtraction was performed on fluorescence image frames, and the mean pixel intensity was calculated for each cell using ImageJ. Baseline cellular GCaMP6s fluorescence was determined immediately prior to drug addition on a per cell basis. Analysis of calcium wave characteristics, such as amplitude, peak number, frequency, and subsequent statistics were performed in R (complete analysis code is available on request). Briefly, calcium response curves were loess fitted (*zoo*) (Zeileis and Grothendieck, 2005), and the local minima and maxima were calculated. A local maximum was considered a peak if its amplitude increased > 35% from its local minimum. Response duration was measured from the onset of the first peak to the end of the last peak. The area under the curve was calculated for the duration of the response. The relationship between dose and the percentage of responding cells was fitted to the following Hill equation: $y = \frac{Top - Bottom}{1+(10)^{(EC_{50}-x)}}$. For each parameter, a linear model was used for two-way ANOVA with Tukey HSD analysis, fitted using virus (mCherry or GNB4), oxotremorine dose, and the interaction of these variables as predictors, as well as the source human sample to consider individual tissue sample variability.

*Luciferase Reporter Pathway Analysis*

PDGFRA$^+$ hOPCs from two patient sources were mixed 1:1 and plated in 96-well tissue culture plates coated with poly-L-ornithine and laminin at $2.5\times10^4$ cells/ml in serum-free media as

described above. 24 hours after seeding, cells were transduced (10 MOI) with Cignal Lenti Luciferase Reporter (Qiagen) for PKC/$Ca^{2+}$ (NFAT, CLS-015L), MAPK/ERK (Elk/SRF, CLS-010L), MAPK/JNK (AP1, CLS-011L), cAMP/PKA (CREB, CLS-002L) or a negative control (CLS-NCL). 24 hours after initial infection, hOPCs were infected with mCherry or GNB4-overexpressing lentivirus (1 MOI). Luminescence responses were quantified 60 hours later using a Promega Bright-Glo reagent in a Bio-Tek plate reader, in accordance with the manufacturer's protocols. Luminescence responses were normalized to the negative control response. The measurements are presented as mean ± SEM for three replicates of two human sample sources.

*Transplantation into shiverer/rag2 mice*

*Animals and surgery.* All experiments using *shiverer/rag2* mice (a gift of Dr. Steven A. Goldman, University of Rochester) (Windrem et al., 2008) were performed according to protocols approved by the University at Buffalo Institutional Animal Care and Use Committee (IACUC). If necessary, newborn pups were genotyped on the day of birth to identify homozygote shiverer mice. hOPCs were cultured for up to 1 week in serum-free media (SFM) containing PDGF-AA/FGF and frozen using ProFreeze (Lonza) prior to surgery. Cells were thawed and then infected 24 hrs later with lentivirus (1 MOI) and allowed to recover for 1-2 days prior to transplantation. Cells were prepared for injection by re-suspending cells in HBSS(-) at $1\times10^5$ cells per µl. Injections were performed as previously described (Sim et al., 2011). Briefly, pups were anesthetized using hypothermia and $5\times10^4$ cells were injected bilaterally into the corpus callosa of postnatal day 2-3 pups. Cells were injected through pulled glass pipettes, inserted directly through the skull. Animals were sacrificed and perfused with saline followed by 4% paraformaldehyde after 8 weeks.

*In vivo immunostaining*. Cryopreserved coronal sections of mouse forebrain (16 µm) were cut and brains were sampled every 160 µm. Immunohistochemistry was performed as described (Sim et al., 2011). Human cells were identified with mouse anti-human nuclei antibody (hNA; 1:100, clone 235-1; Millipore), and sections were stained for MBP (1:400; Abcam, Inc., Cambridge, UK), CC1 (1:50; Millipore), human GFAP (1:800; Covance, Inc., Princeton, NJ, USA), and Ki67 (1:250, Clone SP6, Thermo Scientific). Alexa Fluor-conjugated secondary antibodies (Invitrogen) were used at 1:500.

*Microscopy*. Images were captured at 20× with a motorized fluorescence microscope (Olympus IX-51) using µManager (Edelstein et al., 2010b), and subsequent analyses performed with Fiji (Schindelin et al., 2012). 4-5 sections every 160 µm were sampled from highly engrafted regions in the corpus callosum. Quantification of $hNA^+$ cell density and phenotype was performed by counting cells in midline and lateral regions in the corpus callosum and more than 1,000 cells were counted per animal. $hNA^+$ cells were counted using the ITCN plugin (Byun et al., 2006). The proportion of $hNA^+$ cells expressing CC1, Ki67, and GFAP was determined by manual counting with between 500 and 1,000 cells counted per animal. Confocal microscopy was performed using a Zeiss LSM510 Meta Confocal and analysis was performed in Fiji software. As described previously (Wang et al., 2014), a stack of 40 optical sections was obtained every 0.1 µm, and the number of myelinated fibers that crossed three perpendicular sampling lines, placed randomly across the image, were counted.

## SUPPLEMENTAL REFERENCES


Abiraman, K., Pol, S.U., O'Bara, M.A., Chen, G.D., Khaku, Z.M., Wang, J., Thorn, D., Vedia, B.H., Ekwegbalu, E.C., Li, J.X.*, et al.* (2015). Anti-muscarinic adjunct therapy accelerates functional human oligodendrocyte repair. J Neurosci *35*, 3676-3688.

Alexa, A., Rahnenfuhrer, J., and Lengauer, T. (2006). Improved scoring of functional groups from gene expression data by decorrelating GO graph structure. Bioinformatics *22*, 1600-1607.

Byun, J., Verardo, M.R., Sumengen, B., Lewis, G.P., Manjunath, B.S., and Fisher, S.K. (2006). Automated tool for the detection of cell nuclei in digital microscopic images: application to retinal images. Molecular vision *12*, 949-960.

Cahoy, J.D., Emery, B., Kaushal, A., Foo, L.C., Zamanian, J.L., Christopherson, K.S., Xing, Y., Lubischer, J.L., Krieg, P.A., Krupenko, S.A.*, et al.* (2008). A transcriptome database for astrocytes, neurons, and oligodendrocytes: a new resource for understanding brain development and function. J Neurosci *28*, 264-278.

Du, P., Kibbe, W.A., and Lin, S.M. (2008). lumi: a pipeline for processing Illumina microarray. Bioinformatics *24*, 1547-1548.

Dugas, J.C., Tai, Y.C., Speed, T.P., Ngai, J., and Barres, B.A. (2006). Functional genomic analysis of oligodendrocyte differentiation. J Neurosci *26*, 10967-10983.

Durinck, S., Moreau, Y., Kasprzyk, A., Davis, S., De Moor, B., Brazma, A., and Huber, W. (2005). BioMart and Bioconductor: a powerful link between biological databases and microarray data analysis. Bioinformatics *21*, 3439-3440.

Edelstein, A., Amodaj, N., Hoover, K., Vale, R., and Stuurman, N. (2010a). Computer control of microscopes using microManager. Curr Protoc Mol Biol *Chapter 14*, Unit14.20.

Edelstein, A., Amodaj, N., Hoover, K., Vale, R., and Stuurman, N. (2010b). Computer control of microscopes using microManager. Curr Protoc Mol Biol *Chapter 14*, Unit14 20.

Gentleman, R.C., Carey, V.J., Bates, D.M., Bolstad, B., Dettling, M., Dudoit, S., Ellis, B., Gautier, L., Ge, Y., Gentry, J.*, et al.* (2004). Bioconductor: open software development for computational biology and bioinformatics. Genome Biol *5*, R80.

Geraerts, M., Willems, S., Baekelandt, V., Debyser, Z., and Gijsbers, R. (2006). Comparison of lentiviral vector titration methods. BMC biotechnology *6*, 34.

Hochreiter, S., Clevert, D.A., and Obermayer, K. (2006). A new summarization method for Affymetrix probe level data. Bioinformatics *22*, 943-949.

Jordan, M., Schallhorn, A., and Wurm, F.M. (1996). Transfecting mammalian cells: optimization of critical parameters affecting calcium-phosphate precipitate formation. Nucleic acids research *24*, 596-601.

Konopka, G., Bomar, J.M., Winden, K., Coppola, G., Jonsson, Z.O., Gao, F., Peng, S., Preuss, T.M., Wohlschlegel, J.A., and Geschwind, D.H. (2009). Human-specific transcriptional regulation of CNS development genes by FOXP2. Nature *462*, 213-217.

Langfelder, P., and Horvath, S. (2008). WGCNA: an R package for weighted correlation network analysis. BMC Bioinformatics *9*, 559.

Oldham, M.C., Konopka, G., Iwamoto, K., Langfelder, P., Kato, T., Horvath, S., and Geschwind, D.H. (2008). Functional organization of the transcriptome in human brain. Nat Neurosci *11*, 1271-1282.

Pfaffl, M.W. (2004). Quantification strategies in real time-PCR. In A-Z of Quantitative PCR, S.A. Bustin, ed. (La Jolla, CA: International University Line), pp. 87-112.

Schindelin, J., Arganda-Carreras, I., Frise, E., Kaynig, V., Longair, M., Pietzsch, T., Preibisch, S., Rueden, C., Saalfeld, S., Schmid, B.*, et al.* (2012). Fiji: an open-source platform for biological-image analysis. Nature methods *9*, 676-682.

Sevin, C., Benraiss, A., Van Dam, D., Bonnin, D., Nagels, G., Verot, L., Laurendeau, I., Vidaud, M., Gieselmann, V., Vanier, M.*, et al.* (2006). Intracerebral adeno-associated virus-mediated gene

transfer in rapidly progressive forms of metachromatic leukodystrophy. Hum Mol Genet *15*, 53-64.
Sim, F.J., McClain, C.R., Schanz, S.J., Protack, T.L., Windrem, M.S., and Goldman, S.A. (2011). CD140a identifies a population of highly myelinogenic, migration-competent and efficiently engrafting human oligodendrocyte progenitor cells. Nature biotechnology *29*, 934-941.
Tsai, F.C., Seki, A., Yang, H.W., Hayer, A., Carrasco, S., Malmersjo, S., and Meyer, T. (2014). A polarized Ca2+, diacylglycerol and STIM1 signalling system regulates directed cell migration. Nat Cell Biol *16*, 133-144.
Wang, J., Pol, S.U., Haberman, A.K., Wang, C., O'Bara, M.A., and Sim, F.J. (2014). Transcription factor induction of human oligodendrocyte progenitor fate and differentiation. Proc Natl Acad Sci U S A *111*, E2885-2894.
Windrem, M.S., Roy, N.S., Wang, J., Nunes, M., Benraiss, A., Goodman, R., McKhann, G.M., 2nd, and Goldman, S.A. (2002). Progenitor cells derived from the adult human subcortical white matter disperse and differentiate as oligodendrocytes within demyelinated lesions of the rat brain. Journal of neuroscience research *69*, 966-975.
Windrem, M.S., Schanz, S.J., Guo, M., Tian, G.F., Washco, V., Stanwood, N., Rasband, M., Roy, N.S., Nedergaard, M., Havton, L.A.*, et al.* (2008). Neonatal chimerization with human glial progenitor cells can both remyelinate and rescue the otherwise lethally hypomyelinated shiverer mouse. Cell stem cell *2*, 553-565.
Zeileis, A., and Grothendieck, G. (2005). zoo: S3 Infrastructure for Regular and Irregular Time Series. Journal of Statistical Software; Vol 1, Issue 6 (2005).
Zhang, Y., Chen, K., Sloan, S.A., Bennett, M.L., Scholze, A.R., O'Keeffe, S., Phatnani, H.P., Guarnieri, P., Caneda, C., Ruderisch, N.*, et al.* (2014). An RNA-sequencing transcriptome and splicing database of glia, neurons, and vascular cells of the cerebral cortex. J Neurosci *34*, 11929-11947.